Boundary-Layer Meteorol
https://doi.org/10.1007/s10546-018-0334-x

RESEARCH ARTICLE

Variability of the Mixed-Layer Height Over Mexico City

J. L. García-Franco[1] · W. Stremme[1] · A. Bezanilla[1] · A. Ruiz-Angulo[1] · M. Grutter[1]

Received: 26 April 2017 / Accepted: 4 January 2018

Abstract The diurnal and seasonal variability of the mixed-layer height in urban areas has implications for ground-level air pollution and the meteorological conditions. Measurements of the backscatter of light pulses with a commercial lidar system were performed for a continuous period of almost six years between 2011 and 2016 in the southern part of Mexico City. The profiles were temporally and vertically smoothed, clouds were filtered out, and the mixed-layer height was determined with an ad hoc treatment of both the filtered and unfiltered profiles. The results are in agreement when compared with values of mixed-layer height reconstructed from, (i) radiosonde data, and (ii) surface and vertical column densities of a trace gas. The daily maxima of the mean mixed-layer height reach values > 3 km above ground level in the months of March–April, and are clearly lower (< 2.7 km) during the colder months from September–December. Mean daily minima are typically observed at 0700 local time (UTC $-$ 6h), and are lowest during the winter months with values on average below 500 m. The data presented here show an anti-correlation between high-pollution episodes and the height of the mixed layer. The growth rate of the convective mixed-layer height has a seasonal behaviour, which is characterized together with the mixed-layer-height anomalies. A clear residual layer is evident from the backscattered signals recorded in days with specific atmospheric conditions, but also from the cloud-filtered mean diurnal profiles. The occasional presence of a residual layer results in an overestimation of the reported mixed-layer height during the night and early morning hours.

Keywords Aerosol vertical profile · Lidar · Mexico City · Mixed-layer height · Urban heat island

✉ M. Grutter
grutter@unam.mx

[1] Centro de Ciencias de la Atmósfera, Universidad Nacional Autónoma de México, Mexico City, Mexico

Published online: 01 February 2018

1 Introduction

The diurnal and seasonal variations of the mixed-layer height, which determines the vertical extent of aerosol and gas dispersion, are essential for evaluating pollution episodes, and for characterizing atmospheric dynamics and transport events, which are of crucial importance for air-quality studies. For instance, for simulations of atmospheric-chemistry transport, the height of the convective boundary layer, or mixed-layer height, is an input parameter needed to accurately predict surface concentrations, and to reproduce the dispersion and transport of pollutants (Bossioli et al. 2009). Thus, air-quality models are nowadays useful tools for defining emission-control strategies and aiding in the implementation of adequate legislation in highly populated areas. Moreover, column-mean optical depths measured from satellites or ground-based observatories can be converted into near-surface air-quality information using adequate knowledge of the evolution of the mixed-layer height.

The mixed-layer height is defined by Seibert et al. (2000) as the height above the surface where pollutants are diluted by convection or mechanical turbulence within a time scale of 1 h. The convective boundary layer (or mixed layer), together with a less turbulent residual layer containing former mixed-layer air and a stable nocturnal layer with sporadic turbulence, constitute the planetary boundary layer (PBL).

Mexico City, with over 20 million inhabitants and intense industrial and commercial activities, experiences high levels of air pollution and a poor air quality in general. Even though there are studies reporting the mixed-layer height over Mexico City and its basin (Bossert 1997; Perez Vidal and Raga 2009; Doran et al. 1998; Whiteman et al. 2000; Schaefer et al. 2009), there is no representative long-term study of the mixed-layer height and its evolution. The results of these studies, which are all based on campaigns of short duration, present maximum values of the mixed-layer height of between 2 and 3 km during the afternoon hours. While one study concludes that synoptic-scale flows have strong regional effects on the meteorology and air pollution (Bossert 1997), another shows that the boundary-layer evolution is driven primarily by regional diurnal circulations (Whiteman et al. 2000). A more recent study based on measurements performed from Altzomoni at a high altitude station at a mountain pass nearby Mexico City described how this site, which usually samples free tropospheric air, is influenced by a regional mixed layer during the afternoon hours, regardless of the wind direction (Baumgardner et al. 2009).

Remote-sensing techniques are ideal for long-term studies. Lidar technology for detecting the backscattered signal from pulsed laser has been available for some time, and is used to determine, inter alia, the mixed-layer height during mostly campaign-based studies. Ceilometers are low-cost commercial lidars, which have proven to have substantial advantages over other measurement techniques in boundary-layer studies. These instruments, which are of high spatial and temporal resolution, are robust and eye safe, and require little maintenance. Since 2008, a ceilometer (Vaisala CL31) has been in almost continuous operation in the southern region of Mexico City. Here, the retrieved mixed-layer heights are compared with independent measurements, and the mean diurnal and annual cycles over this site are reported.

2 Instrumentation

Presented here are the measurements from three instruments located at the same site, but each using a different technique. The vertical profiles of backscattered laser signals were obtained from a commercial lidar. Carbon monoxide (CO) concentrations near the surface were mea-

sured with an in situ gas analyzer, and the total column density of CO was retrieved from solar absorption measurements made with an infrared spectrometer. These last two datasets were used to reconstruct the mixed-layer height with which to compare the lidar results. The measurements were all performed at the site of the Universidad Nacional Autónoma de México (UNAM) (19.3262°N, 99.1761°W, 2280 m above sea level (a.s.l.)), which belongs to the University Network of Atmospheric Observatories (RUOA, http://www.ruoa.unam.mx). This research facility is located on the rooftop of the Center of Atmospheric Sciences building within the UNAM campus in southern Mexico City.

2.1 Ceilometer

The vertical profiles of the backscattered laser signal were measured with a Vaisala CL31 ceilometer based on the lidar technique, which uses light pulses sent to the atmosphere from a laser source, and, in its simplest form, measures the returned intensity of elastically-scattered light at different distances. Ceilometers have been widely used to obtain the height of the cloud base, the vertical visibility and the cloud cover. However, these devices can also be used to retrieve other atmospheric parameters of interest such as aerosol profiles and the mixed-layer height (Eresmaa et al. 2006).

The Vaisala CL31 ceilometer uses an indium-gallium-arsenide pulsed-diode laser emitting 910 nm pulses at a repetition rate of 10 kHz, and uses a single lens for transmitting and receiving the light. The centre of the lens is used for collimating the outgoing laser beam, while the outer part of the lens is used for focusing the incoming light. The receiver consists of a silicon avalanche photodiode, and an interference filter with a central wavelength of 915 nm and a 50% band-pass width of 36 nm. The maximum detectable cloud-base height of this instrument is 7500 m above ground level (a.g.l). Backscattered profiles may be recorded every 2 to 120 s at a maximum vertical resolution of 10 m.

The acquisition rate was set to record profiles every 16 s, and the parameters were changed from the original factory settings to optimize the detection of aerosols (Christoph Münkel, personal communication, 2008). To increase the signal-to-noise ratio, the raw profiles were initially smoothed by performing a moving average, and, if at least 50% of the data were available, a working profile every 10 min was created. The vertical structure of the profiles was also smoothed with an altitude-dependent smoothing kernel, which was applied to ensure high resolution near the surface, and averaged over a greater number of neighbouring points at higher altitudes. Therefore, profiles with a 10-m spatial resolution are convoluted with Gaussian-like functions, enabling us to maintain the same number of data points for each profile. For altitudes of between 200 and 4000 m, the half-widths of the Gaussian functions range from 50 to 180 m.

2.2 In Situ Gas Analyzer

Carbon monoxide (CO) surface measurements at the UNAM site are routinely performed with a cavity ring-down spectrometer by Picarro Inc., model G2401. This in situ analyzer is capable of carrying out simultaneous measurements of CO_2, CO, CH_4 and H_2O, while providing the level of precision needed to meet the standards of the Global Atmospheric Watch program of the World Meteorological Organization. The manufacturer reports a precision of < 1.5 ppb for 5-min averages of CO concentration in the absence of routine calibrations with a certified gas standard.

The spectrometer is a sophisticated time-based device, which uses a laser to quantify the spectral features of gas-phase molecules in an optical cavity, and operates with an effective

optical path of up to 20 km in a compact cavity. The analyzer uses a high-precision-wavelength monitor to avoid any drift in the laser, and to maintain the absolute spectral position and an accurate peak quantification. A wavelength monitor ensures that only the special features of interest are incorporated into the analysis, which reduces the sensitivity to any interfering species. Precise temperature and pressure controls are integrated to guarantee the fidelity of the measurements.

While concentrations of the gases and other parameters are recorded twice per second, 5-min averages are used to obtain the surface concentration of CO; data from this instrument are available from July 2014.

2.3 Solar Absorption Infrared Spectrometer

The total CO column density [molecules cm^{-2}] over the UNAM site is obtained from spectrally resolved solar-absorption measurements using a Fourier transform infrared (FTIR) spectrometer coupled to an in-house solar tracker (Bezanilla et al. 2014). The infrared spectra of 0.075-cm^{-1} resolution are measured with an FTIR spectrometer (Bruker Optics, model Vertex80) equipped with a KBr beam splitter, and ZnSe windows. The mid-infrared region is used to detect the CO absorption lines recorded using a liquid-nitrogen cooled, mercury-cadmium-telluride detector, and a band-pass filter. The CO column density is analyzed in three spectral windows (2056.70–2059.00, 2068.56–2069.77 and 2156.50 − 2160.15 cm^{-1}) using H_2O, CO_2, O_3, OCS and N_2O as interference gases for the fits following the strategy described by Stremme et al. (2009). The CO total column data are available from July 2010, with some periods of interruption due to maintenance work.

3 Analysis

3.1 Detection of Clouds and Precipitation

Precipitation and clouds are important sources of error in the determination of the mixed-layer height from backscattering measurements. The radiative properties of cloud and rain droplets make them impenetrable for the 910-nm photons from the lidar, since virtually all the radiation is scattered. Profiles of large reflectivity values during rain events and low or high clouds can thus result in the calculation of unrealistic values of the mixed-layer height. For these reasons, the collected data were filtered for clouds and precipitation using the algorithm reported by Teschke et al. (2008), which uses statistical parameters to detect clouds and precipitation by first normalizing the backscattered signal by its variance, highlighting the particular altitudes where clouds are present. Using the global mean μ and variance σ, an empirical threshold for each pixel is defined by

$$B(z,t) < \mu + 3\sqrt{\sigma}, \tag{1}$$

where the inequality in Eq. 1 is, as stated by Teschke et al. (2008), the result of a simple empirical estimate. Basically, it fulfils two goals, while filtering clouds and precipitation. Firstly, it enables manipulation of the spatial and temporal ranges over which the mean and variance are calculated. Secondly, the procedure filters clouds and particularly rain events efficiently, while not eliminating those events with a strong backscattered signal because of a large aerosol loading. In particular, the coefficient's value of 3 in this equation has been tested and proven to be adequate, where values of 2 or 4, for example, have been shown to be either too strict or too lenient. In short, this method enables us to obtain the mixed-layer height

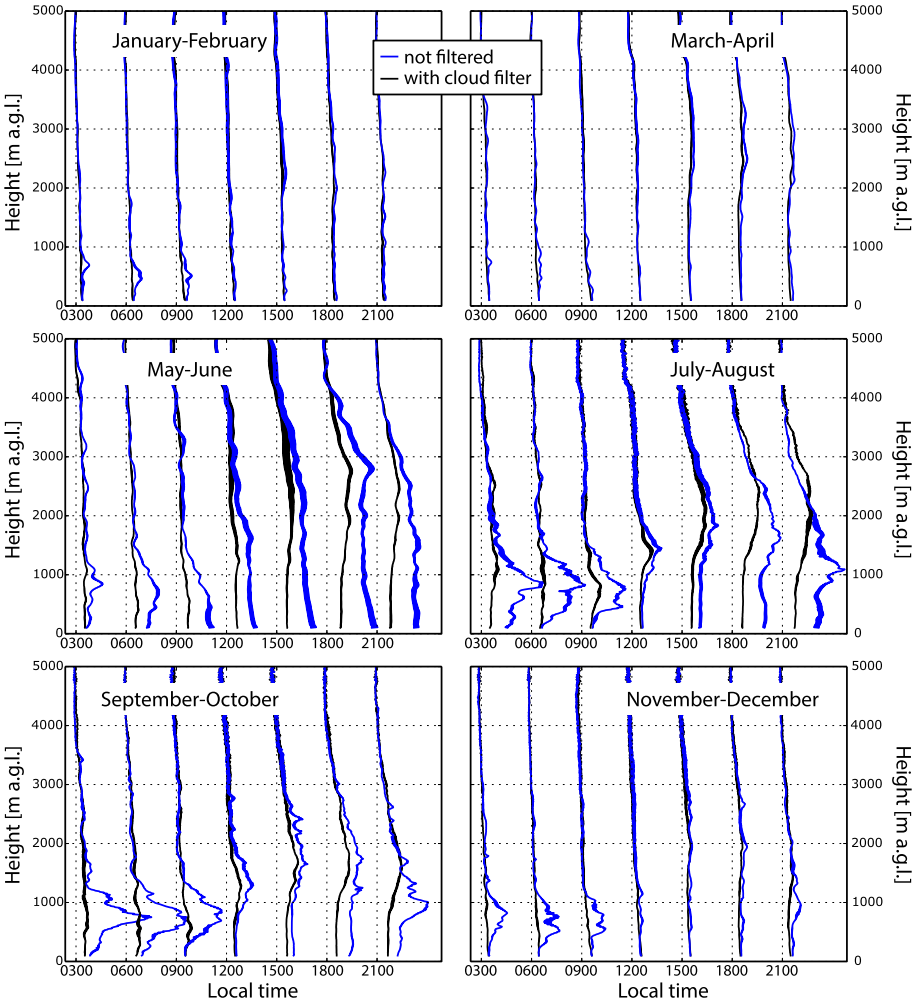

Fig. 1 Averaged bi-monthly vertical profiles of backscatter shown every 3 h. No cloud filter was applied to the profiles in blue, but the profiles in black have been filtered. The backscattering intensity has arbitrary units, and is presented in equivalent scales throughout the six panels

in cloud-free conditions for comparison with those from the complete database without the application of any filter.

Using this procedure, the backscattering data have been filtered for clouds and precipitation. Figure 1 presents the average backscattering profiles for the entire measurement period (2011–2016) for specific hours of the day. Indicated in blue are the smoothed profiles as described above without any further processing, while those in black are the average profiles after omission of those not fulfilling the condition given by Eq. 1. Each panel in Fig. 1 corresponds to the average over a two-month period to emphasize clear differences between the dry (November–April) and rainy (May–October) seasons. Of all collected profiles, 45% are classified as being affected by clouds or precipitation, with the rest considered to be undisturbed by clouds. Mean mixed-layer heights were then computed for both sets of data.

3.2 Mixed-Layer-Height Retrieval

The mixed-layer heights were retrieved between 150 and 4000 m using a combined algorithm based on the gradient method described by Münkel (2007), and the method of wavelet-covariance transform described by Grabon et al. (2010). For the first case,

$$h = \min\left(\frac{\partial B(z)}{\partial z}\right) = \max\left(-\frac{\partial B(z)}{\partial z}\right), \tag{2}$$

where h refers to the mixed-layer height, $B(z)$ is the backscattering intensity in arbitrary units, and z is the height. The wavelet-transform method uses a Haar wavelet to compute the coefficients for a particular dilation (a) and translation or location (b) throughout the backscattering profile $B(z)$, where

$$W_f(a,b) = \frac{1}{a}\int_{z_0}^{z_f} B(z)H\left(\frac{z-b}{a}\right), \tag{3}$$

and where the function H is a reference to the Haar-wavelet function evaluated at the points a and b. The mixed-layer height here is defined as the maximum W_f present. It is noteworthy that, with the use of the Haar wavelet, Eq. 3 can represent a simple gradient relation for a particular a and b, making its interpretation similar to Eq. 2. As specified by Grabon et al. (2010), this is an iterative approach, where the window of interest, in this case defined by the dilation a, becomes iteratively narrower, and thus at the first attempt cannot produce a mixed-layer height equal to the lowest possible value. Therefore, the wavelet-transform method complements the gradient method, since the latter can produce floor values or false hits.

The algorithm first locates the height given by the largest negative gradient found among adjacent heights, with two possible false hits identified: the floor values, i.e. the minimum value possible, which in this case is 150 m, and a rapid change, increase or decrease, in the values of the mixed-layer height between two adjacent timesteps. A threshold of 400 m for a timestep of 10 min was established, which corresponds to a growth or decay rate of 2.4 km h^{-1}. As shown below, typical growth rates are on average 600 m h^{-1} during the late morning period, with values above this threshold, therefore, considered to be unrealistic. The intention of setting this threshold is to eliminate rare large and sudden changes in adjacent values of the mixed-layer height; these have only a minor effect on the monthly averages, or the mean diurnal evolution of the mixed-layer height.

If the mixed-layer height given by the gradient method is characterized as a false hit, then the wavelet-transform method computes a second height using an iterative approach to narrow the window of the profile to avoid any further floor false hits. For the cases in which the first approach reports a false hit due to a floor value, then the reported mixed-layer height is given solely by the wavelet-transform method. For the other case when the gradient method reports a large change between adjacent values ($>$ 400 m), then there are two possibilities. If the value reported by the wavelet-transform method also presents a large step with respect to the previous value, then the arithmetic mean of the two methods is calculated. Otherwise, the wavelet-transform height is reported as the mixed-layer height for that timestep. It should be noted that, consistent with Helmis et al. (2012) and Lotteraner and Piringer (2016), no distinction is made in this algorithm between stable and convective situations.

3.3 Radiosonde Intercomparison

Daily radiosonde data from the Mexican National Weather Service are available from balloon soundings launched at 0600, 1200 and 1800 local time (UTC − 6h) from Tacubaya in Mexico City (19.404°N, −99.196°E, 2308 m a.s.l.), which is less than 15 km away from the UNAM site. Not every day delivers data for all three periods, and the launch at noon is infrequent. The balloon data were processed to retrieve the mixed-layer height using the standard Richardson-number method, which, as described in Piringer et al. (2007), can be used for all atmospheric conditions and, as such, is used for all the available sounding data. The gradient Richardson number Ri (Joffre et al. 2001) is given by

$$Ri(z_{i+1}) = (g/T_s)\frac{(\theta_{i+2} - \theta_i)(z_{i+2} - z_i)}{(u_{i+2} - u_i)^2}, \tag{4}$$

where g is the acceleration due to gravity, z is the height a.g.l., T_s and θ are the surface and potential temperatures [K], respectively, and u is the wind speed.

To compare the datasets from coincident times, soundings were only used if the lidar data were available for the same day at the same time. Soundings were only considered if enough values were available within the boundary layer based on a mean resolution threshold of 500 m in the region between 150 and 4000 m. For this period, 526, 66 and 371 matching cases were found for the three launch times, respectively. The mixed-layer height from the lidar profiles was obtained by the method described above, and averaged over a 1-h window. For example, to establish the value at 0600 local time, the mean mixed-layer height between 0530 and 0630 was reported as the mixed-layer height to be analyzed.

Richardson numbers were calculated for all heights of soundings between 100 and 4000 m, where the first encountered value above the ground of the critical Richardson number ($Ri_c = 0.25$) in the profile is determined as the level of the mixed layer.

Figure 2 shows a scatter plot of the mixed-layer height calculated by the two methods and instruments described above. A coefficient of $r = 0.49$ reveals little correlation, particularly for the greater mixed-layer heights corresponding to the afternoon launches shown as green dots.

The summary of this intercomparison is shown in Table 1, where the mean, median and standard deviation (σ) of the mixed-layer height for the 0600, 1200 and 1800 launches are reported. Note that the largest discrepancies are seen for the launches at noon, which are

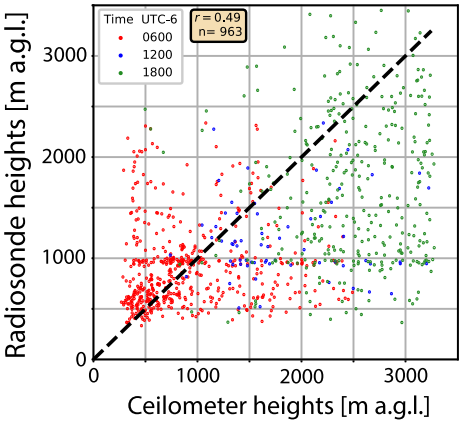

Fig. 2 Scatter plot comparing hourly mean mixed-layer heights computed from the ceilometer data with those from radiosondes launched at 0600, 1200 and 1800 (UTC − 6h) as shown in red, blue and green, respectively. The dashed line corresponds to the 1:1 correlation

Table 1 Comparison of mixed-layer heights obtained from the lidar and radiosonde methods

Method	Local time	Mean (m)	Median (m)	σ (m)
Lidar	0600	930	750	540
Radiosonde	0600	910	810	410
Lidar	1200	1860	1640	630
Radiosonde	1200	1190	1110	390
Lidar	1800	2550	2580	580
Radiosonde	1800	1720	1620	760

scarce, and have the lowest number of coincident values. The morning values give the most similar results, while for the afternoon launches, the mixed-layer heights inferred from the radiosonde data are generally lower and present a larger standard deviation.

3.4 Comparison of Mixed-Layer Height with the Trace-Gas Method

An alternative estimate of the mixed-layer height is also generated from the continuous measurement of a trace gas both at the surface and in the vertical column within the mixed layer, provided that the gas is not highly reactive and is homogenously distributed throughout the lowest layer. This assumption provides a simple approximation of the mixed-layer height, and has been proven to be valid for CO as the trace gas through the procedure described by Stremme et al. (2009). The method consists of using the measurements at the UNAM site for CO surface concentrations as described in Sect. 2.2, and the total CO vertical column density from infrared spectroscopic measurements of solar absorption (Sect. 2.3).

The measured CO total column density can be divided into the integrated concentration of the gas through the mixed layer (from the ground to the unknown value of the mixed-layer height), and the background CO concentration above the mixed layer, which is fairly constant and varies only according to the season. This parameter is known from measurements performed daily at the nearby, high-altitude atmospheric observatory in Altzomoni (19.119°N, 98.655°W, 3,985 m a.s.l.) with a high-resolution infrared spectrometer, which contributes to the Network for the Detection of Atmospheric Composition Change (https://www2.acom.ucar.edu/irwg). The background CO concentration is thus precisely known and subtracted from the total column density measured at the UNAM site for calculation of the mixed-layer height, which is limited to daytime and clear-sky conditions, since the column measurement requires the sun.

Two typical examples of the variability of the mixed-layer height as calculated with the CO trace-gas method are shown as red dots in Fig. 3. Each plot corresponds to a one-day time series of the backscattering profile measured with the ceilometer system at the UNAM site with a false colour scale representing the intensity of the backscattered signal in arbitrary units. Superimposed on each plot are white dots representing the mixed-layer height determined from ceilometer data with the method described in Sect. 3.2. In Fig. 3a, corresponding to 9 November 2015, low cloud is present in the early morning, and the convective mixed layer increases thereafter to a height of approximately 2000 m a.g.l.. In the afternoon, clouds develop, preventing the determination of a mixed-layer height from either method (cloud filter applied and no sun for the trace-gas method). However, during the morning period without clouds, the reconstructed mixed-layer heights from the CO measurements (red dots) follow the growth of the ceilometer well. However, the estimates of the mixed-layer height

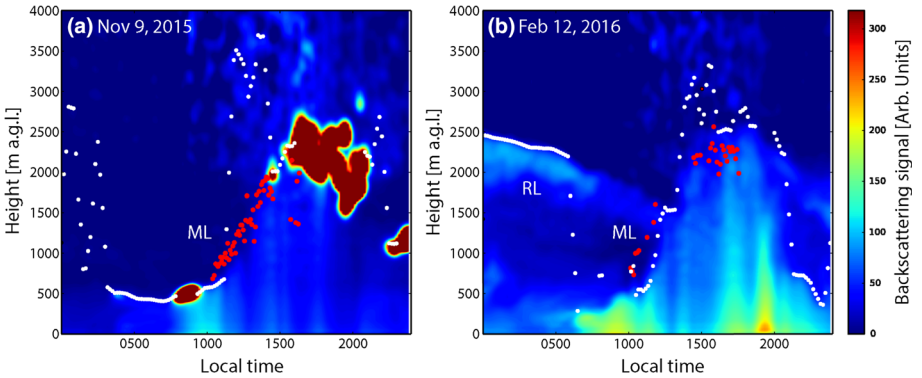

Fig. 3 Diurnal backscattering profiles (arbitrary units) for selected days with retrieved mixed-layer heights from lidar data (white dots) and the CO trace-gas method (red dots). The left panel **a** corresponds to 9 November 2015 and **b** to 12 February 2016. ML: mixed layer, RL: residual layer

Fig. 4 Correlation between the mixed-layer heights calculated from the trace-gas method and those from backscattering profiles. The 1:1 correlation is shown with the dashed line, while the solid black line is the linear regression forced to the origin. The dots are coloured with respect to the corresponding surface CO concentration at the time of the coincident measurements

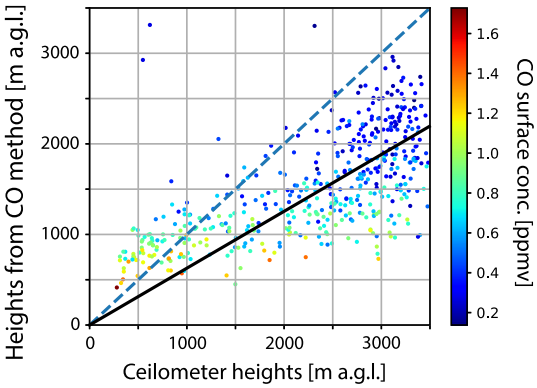

from the backscattering signals fail at certain times during the night, and also just before the formation of afternoon clouds.

On 12 February 2016 (Fig. 3b), both mixed-layer-height products show a similar behaviour for the period between 1000 and 1700 local time when the mixed-layer height according to the CO measurements (red dots) is available. Here, the mixed layer reaches heights above 2500 m a.g.l., with strong backscattered signals detected near the surface. A large aerosol loading is responsible for the strong lidar signals observed on this day, and is typical for this time of the year when thermal inversions prevent the ventilation of pollution in the city. Moreover, the presence of a residual layer is clearly visible from the backscattered signals descending throughout the night until the early morning. This elevated airmass either contains pollutants from the day before, or has been transported from another region, and is falsely identified as the mixed-layer height from our algorithm. Further discussion of the residual layer and its affect on the average diurnal variability follows below.

Mixed-layer heights derived from the trace-gas method are plotted against mixed-layer heights obtained from ceilometer profiles in Fig. 4 for those days between February 2015 and May 2016 containing column CO measurements. The 499 coincident 1-h averages return a Pearson correlation coefficient of $r = 0.64$ and a slope of 0.63 for a linear regression fit forced through zero. Furthermore, the plot has been coloured with respect to the CO concentration

measured at the surface for each individual estimation of the mixed-layer height. Analysis of this comparison reveals several features of the methods employed to estimate the height of the mixed layer.

Figure 4 clearly demonstrates that the highest ground-level CO concentrations, which are depicted with warmer colours, correspond to the smaller mixed-layer height, which is consistent with the degree of urban pollution, the strength of the advection of pollutants from the basin, as well as the height of the mixed layer.

Moreover, the mixed-layer height calculated from the trace-gas method is underestimated above a certain height, which may be related to the use of three distinct datasets for its estimation. We have calculated the average ratio between the mixed-layer height from both the trace-gas and ceilometer methods (h_{CO}/h_{ceilo}) for three altitude ranges: the complete range (0–4000 m a.g.l.), the layer below Altzomoni (0–1700 m a.g.l.), and 1700–4000 m a.g.l. We find average h_{CO}/h_{ceilo} obtained for the three altitude ranges of 0.78, 1.15, and 0.73, respectively, which reveals that, for mixed-layer heights below the height of the Altzomoni station, an improved correspondence between the methods is obtained. The overall underestimation of the mixed-layer height as described by the solid line in Fig. 4 is apparent for mixed-layer heights larger than 1700 m, because the CO column density above the high-altitude station at Altzomoni is subtracted from that measured within the city, leading to smaller column density, and thus to lower calculated heights for the same surface concentration. While this situation is expected to occur during those afternoons when the Altzomoni station is submerged in the regional mixed layer as documented by Baumgardner et al. (2009), the trace-gas method yields good results during the growing phase corresponding to the morning and early afternoon hours.

4 Results

For the period between January 2011 and April 2016, lidar backscattering data were collected at the UNAM station of the RUOA network, which is located at the Center for Atmospheric Sciences within the UNAM campus in Mexico City. The profiles were smoothed in time and space, as described in Sect. 2.1, enabling the retrieval of the mixed-layer height, from which diurnal means and long-term time series were generated. An ad hoc cloud filter was applied to the data (Sect. 3.1), with the results compared with the unfiltered profiles. Here, the average mixed-layer height from 2011 to 2016 as representative of the southern regions of the city is presented, including the bi-monthly variability of the backscattering profiles, and the diurnal and inter-annual behaviour of mixed-layer heights.

4.1 Backscattering Profiles

Typical profiles of the backscattering signals averaged over a period of two months during the entire measurement period are shown in Fig. 1, where the blue lines represent the average profiles of unfiltered data, and the black lines are cloud-filtered profiles at different times of the day. The use of a cloud and precipitation filter enables assessment of the impact of the filter on the average evolution of the mixed-layer height, and clearly shows the effect of clouds in the reported profiles, particularly during the rainy season from May to October. The months from January to April have less cloud interference in the backscattering signals, since the filtered and raw profiles look very similar, which is consistent with its being the dry season. For example, the period from July to August has remarkable differences during the night, while the January–February profiles show relatively smaller differences.

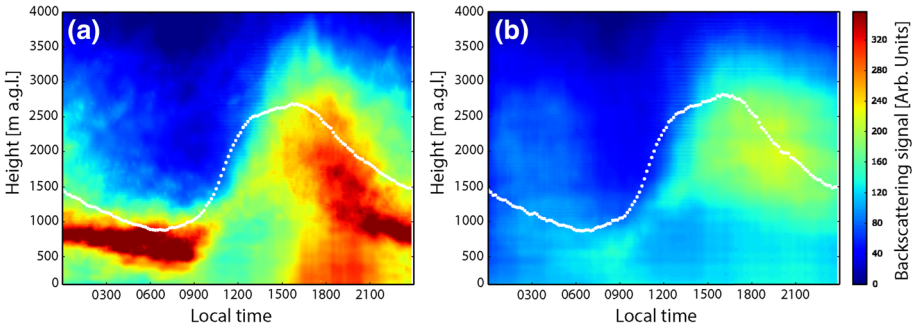

Fig. 5 Average diurnal variation of backscattered signal (2011–2016). Panel **a** without and **b** with cloud filter. The white dots represent the mean values of the mixed-layer height calculated for 10-min windows for the entire period. Time is in standard local time covering an entire day

The diurnal evolution of the average backscattering profiles for the entire measurement period is presented in Fig. 5, showing averaged profiles in colour scales without removal of the effect of the clouds (a) and after application of the cloud filter (b). For clarity, the colour scale in both plots is set to a fixed value. The raw averaged data show intense signals associated with clouds starting at around 2000 local time descending from about 1 km a.g.l. to 500–600 m before sunrise. The growth of the mixed layer starting at around 0900 to heights above 2.5 km is also clearly seen in this plot. After implementing the cloud filter shown in Fig. 5b, a smooth layer is clearly evident in the day representing a statically stable residual layer, which is not expected to be visible on all the days from the backscattering data, but is clearly observed in particular events as shown in Fig. 3b. The plot with the filtered backscattered signals more clearly shows the monotonic increase and diurnal growth of the mixed layer.

4.2 Mixed-Layer Height

The mixed-layer height was estimated following the method described in Sect. 3.2. The ceilometer-derived mixed-layer heights were used to build a large dataset, and construct a climatology of the mixed-layer-height evolution in time, for which it is possible to obtain the bi-monthly diurnal evolution and their mean anomalies, as well as the inter-annual variability of the mixed-layer-height maxima and growth rates.

4.2.1 Diurnal Evolution

Figure 5b shows the characteristic diurnal evolution of the mixed-layer height (white, dotted line) calculated by averaging all values of the mixed-layer height retrieved from the 10-min-filtered profiles according to the algorithm described in Sect. 3.1, and represents the mean evolution of the mixed-layer height for cloud-free conditions throughout the entire measurement period. On average, the mixed-layer height has a maximum mean value of 2750 m occurring at around 1600 local time and a minimum value of 850 m occurring at 0700 local time. The calculation from unfiltered profiles tends to produce values of the mixed-layer height 130 m lower at its maximum on average, while at the minimum value, the results are very similar for cloud-free conditions. However, the difference in the diurnal evolution of the mixed-layer height between filtered and non-filtered profiles can be significant on single days, particularly during cloudy and rainy periods.

Based on the mixed-layer-height database corresponding to cloud-free conditions, the bi-monthly diurnal evolution over Mexico City is shown in Fig. 6a, with sets of 2 months plotted

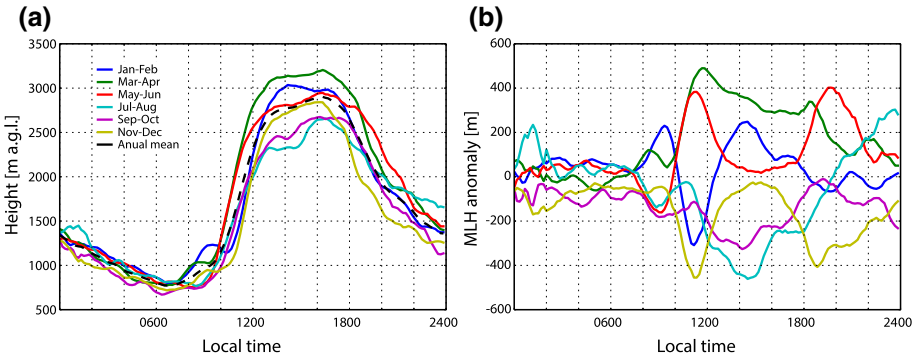

Fig. 6 Mean diurnal evolution of **a** the mixed-layer height and **b** mixed-layer-height anomaly for cloud-free conditions in sets of two-month averages

in different colours starting in January–February. While a similar structure is observed for all curves, different features are evident according to the season of the year, illustrating that the mixed-layer height starts to grow earlier for the months March–June, followed by the July–August curve. Note that all data are reported in local winter time. Also expected are those curves illustrating the latest onset for the convective growth starting after 1000 local time consistent with the late-autumn/winter months of November to February.

The highest values of the mixed-layer height are observed to reach mean values above 3 km a.g.l in March–April, which are typically the warmest and driest months of the year. Significantly lower mean maximum values of the mixed-layer height are obtained during the July–October months, which coincide with the season of highest precipitation.

4.2.2 Mixed-Layer-Height Anomaly

The mean diurnal evolution of the mixed-layer height is relatively similar throughout the year, with the averaged bi-monthly differences more pronounced in terms of the estimated anomaly with respect to the mean mixed-layer height as shown by the dashed line in Fig. 6a. The anomaly is calculated as the difference between the bi-monthly average and the mean diurnal evolution throughout the year as shown in Fig. 6b, which indicates a seasonal cycle of anomalies, varying from positive to negative values, including a quasi-neutral period. The anomalies show departures from the mean values of mixed-layer height during the growing phase as large as 500 m. The curves corresponding to the period between March and June indicate clear positive anomalies, which is indicative of stronger convection. The negative anomalies correspond to the period between July and October, and occur mostly in the afternoon. A special case for the November–February period is evident, when a negative anomaly is observed at the beginning of the growing phase of the mixed-layer height due to the later sunrise, and followed by a positive anomaly during the afternoon. This pattern is inverted during the warmer months (July–October), and probably can be attributed to the typical thermal inversions over Mexico City during the winter months.

4.2.3 Long-Term Trends

The continuous data collected during the reported period enable the representation of the seasonal cycle of the mixed-layer height as a time series in Fig. 7 using three metrics. Both

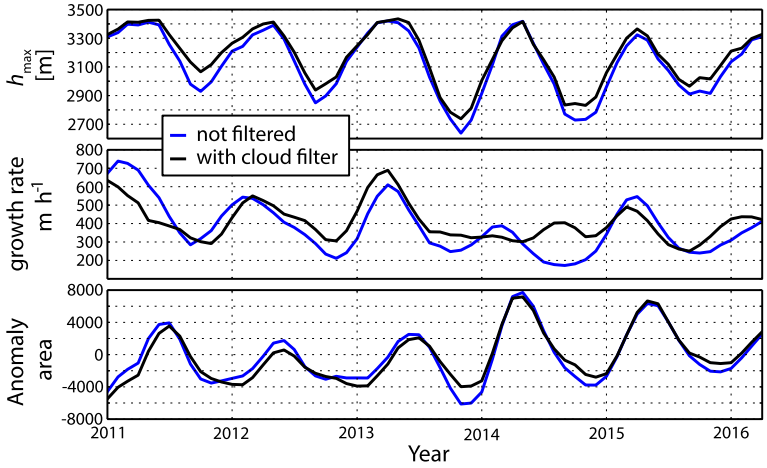

Fig. 7 Time series of monthly averages of the daily maximum (upper) of the mixed-layer height during the entire period. Also shown are the growth rates (middle) and anomaly areas (bottom) of the monthly-averaged mixed-layer height calculated from unfiltered (blue) and cloud-filtered (black) backscattering profiles

mixed-layer heights resulting from the monthly-averaged unfiltered data and those with cloud-free conditions are shown in black and blue, respectively. A clear seasonal cycle is observed for the average daily maximum values ($h_{\max}$), with a peak around April–June and a minimum around September–November, and some year-to-year variability, which is generally consistent between the unfiltered and cloud-filtered datasets. The inter-annual amplitude in the $h_{\max}$ values is observed to vary between 300 and 700 m, and is affected mostly by the lower values during Autumn. As there is no clear cycle or seasonality of the daily minimum value of the mixed-layer height, it is not shown.

The maximum value ($h_{\max}$) throughout the years remains similar with a slight decrease from 2015–2016, but reached a significantly low value in 2013, before increasing in the following years. The reported observed period is limited in the sense that it is not long enough to be correlated with large-scale atmospheric phenomena, such as the El Niño-Southern Oscillation, although some annual variability might be explained by such factors.

The average growth rates are calculated for every month in the time series, and are presented in the middle panel of Fig. 7. The annual cycle follows a similar pattern as $h_{\max}$, suggesting that, during the warmer months, the mixed layer grows more rapidly due to the stronger convection. The minimum values in the time series of the growth rate are more consistent with the minima in the plot of $h_{\max}$ values. Another metric showing a clear annual cycle is the area of the monthly anomaly, which is calculated from the anomalies shown in Fig. 6b, but for the individual months rather than as an average of the entire measurement period. The anomaly area corresponds to the sum of all positive or negative values, and calculated for all hours of the day. Positive values imply greater mixed-layer heights on average than the mean value obtained for each particular month. The anomaly area time series in the lower panel of Fig. 7 indicate maxima during the March–June period, which is consistent with that demonstrated in Fig. 6b. Here, the years of 2012 and 2013 stand out as having lower anomaly areas than other years in the time series. Other interesting things to notice are the minimum values in the monthly anomaly areas, which have been consistently growing in the past six years. A possible explanation for this could be a larger heat-island effect caused by the rapid changes of the urban environment of Mexico City. The extent of the city and its

morphological characteristics, with large growth indices in terms of the construction, traffic, emissions and population, may influence the dynamics of the atmosphere close to the surface as suggested by the lower panel in Fig. 7.

5 Conclusions

We have presented more than six years of backscatter data from lidar measurements in Mexico City. The profiles have been averaged in time and height to demonstrate the characteristic diurnal and seasonal variabilities of this urban environment. An algorithm to retrieve mixed-layer heights from the backscattering signals was developed, and filtering of the profiles enabled evaluation of the effect of clouds and precipitation in calculations of the mixed-layer height. The backscatter signals show the presence of a residual layer during the early hours of some of the days, which contains aerosols and gaseous pollutants from either local sources from previous days, or from other sources, such as from biomass burning transported from other regions. Unfortunately, our current mixed-layer-height detection algorithm is unable to separate the residual layer from the thermally-driven convective mixed layer. Our reported mixed-layer heights are, therefore, affected during the night and early morning hours by the eventual presence of the residual layer.

The mixed-layer heights have been compared with radiosonde data and with an independent mixed-layer-height calculation from simultaneous measurement of the surface and vertical column density of a trace gas. The results confirm that the mixed-layer height derived from the continuous lidar measurements is accurate to within 15% during both its growing phase and until the late afternoon hours (0600–1800 local time) when compared with the trace-gas method. The mean diurnal evolution of the mixed-layer height shows a maximum mean value of 2750 m occurring at around 1600 local time and a minimum value of 850 m occurring at 0700 local time A clear anti-correlation has been found between the high pollution levels and the height of the mixed layer. The annual cycle of the mean daily maxima has an amplitude of up to 700 m and peak values during the warmest months (March–April). The time series of our calculated monthly anomalies from the mean suggest that during the last six years, there has been an increasing trend of reduced values observed during the winter months. This result may be related to a more intense heat-island effect caused by urban growth and its associated activities. This is, nevertheless, the first long-term study based on observations describing the evolution of the mixed-layer height over Mexico City.

Acknowledgements This investigation was funded by DGAPA-UNAM Grant No. IN107417 and Conacyt Nos. 249374 & 275239. The RUOA network (Red Universitaria de Observatorios Atmosféricos) from the Universidad Nacional Autónoma de México is acknowledged for making the data available, with technical support from D. Flores, O. López, W. Gutiérrez, M. García and M.A. Robles. We thank I. Ortega for discussions and T. Blumenstock and F. Hase from the KIT for their cooperation in setting up the NDACC site in Altzomoni.

References

Baumgardner D, Grutter M, Allan J, Ochoa C, Rappenglueck B, Russell L, Arnott P (2009) Physical and chemical properties of the regional mixed layer of mexico's megapolis. Atmos Chem Phys 9(15):5711–5727

Bezanilla A, Krueger A, Stremme W, Grutter M (2014) Solar absorption infrared spectroscopic measurements over Mexico City: methane enhancements. Atmósfera 27(2):173–183

Bossert JE (1997) An investigation of flow regimes affecting the Mexico City region. J Appl Meteorol 36(2):119–140

Bossioli E, Tombrou M, Dandou A, Athanasopoulou E, Varotsos KV (2009) The role of planetary boundary-layer parameterizations in the air quality of an urban area with complex topography. Boundary-Layer Meteorol 131(1):53–72

Doran JC, Abbott S, Archuleta J, Bian X, Chow J, Coulter R, de Wekker SFJ, Edgerton S, Elliott S, Fernandez A, Fast JD, Hubbe JM, King C, Langley D, Leah J, Lee JT, Martin TJ, Martinez D, Martinez JL, Mercado G, Mora V, Mulhearn M, Pena JL, Petty R, Porch W, Russell C, Salas R, Shannon JD, Shaw WJ, Sosa G, Tellier L, Templeman B, Watson JG, White R, Whiteman CD, Wolfe D (1998) The IMADA-AVER boundary layer experiment in the Mexico City area. Bull Am Meteorol Soc 79(11):2497

Eresmaa N, Karppinen A, Joffre SM, Räsänen J, Talvitie H (2006) Mixing height determination by ceilometer. Atmos Chem Phys 6(6):1485–1493. https://doi.org/10.5194/acp-6-1485-2006

Grabon JS, Davis KJ, Kiemle C, Ehret G (2010) Airborne lidar observations of the transition zone between the convective boundary layer and free atmosphere during the International H2O Project (IHOP) in 2002. Boundary-Layer Meteorol 134(1):61–83

Helmis C, Sgouros G, Tombrou M, Schäfer K, Münkel C, Bossioli E, Dandou A (2012) A comparative study and evaluation of mixing-height estimation based on sodar-rass, ceilometer data and numerical model simulations. Boundary-Layer Meteorol 145(3):507–526

Joffre S, Kangas M, Heikinheimo M, Kitaigorodskii S (2001) Variability of the stable and unstable atmospheric boundary-layer height and its scales over a boreal forest. Boundary-Layer Meteorol 99(3):429–450

Lotteraner C, Piringer M (2016) Mixing-height time series from operational ceilometer aerosol-layer heights. Boundary-Layer Meteorol 161(2):265–287

Münkel C (2007) Mixing height determination with lidar ceilometers-results from Helsinki testbed. Meteorol Z 16(4):451–459

Perez Vidal H, Raga G (2009) On the vertical distribution of pollutants in Mexico City. Atmósfera 11(2):95–108

Piringer M, Joffre S, Baklanov A, Christen A, Deserti M, De Ridder K, Emeis S, Mestayer P, Tombrou M, Middleton D, Baumann-Stanzer K, Dandou A, Karppinen A, Burzynski J (2007) The surface energy balance and the mixing height in urban areas—activities and recommendations of COST-Action 715. Boundary-Layer Meteorol 124(1):3–24

Schaefer K, Flores-Jardines E, Emeis S, Grutter M, Kurtenbach R, Wiesen P, Müenkel C (2009) Determination of mixing layer heights by ceilometer and influences upon air quality at Mexico City airport. Proc SPIE 7475(74):750M

Seibert P, Beyrich F, Gryning SE, Joffre S, Rasmussen A, Tercier P (2000) Review and intercomparison of operational methods for the determination of the mixing height. Atmos Environ 34(7):1001–1027

Stremme W, Ortega I, Grutter M (2009) Using ground-based solar and lunar infrared spectroscopy to study the diurnal trend of carbon monoxide in the Mexico City boundary layer. Atmos Chem Phys 9(20):8061–8078. https://doi.org/10.5194/acp-9-8061-2009

Teschke G, Reichardt J, Engelbart D (2008) Wavelet algorithm for the estimation of mixing layer height with ceilometers. In: Reviewed and revised papers presented at the 24th international laser radar conference (ILRC), Citeseer, pp 23–27

Whiteman CD, Zhong S, Bian X, Fast J, Doran J (2000) Boundary layer evolution and regional-scale diurnal circulations over the Mexico Basin and Mexican plateau. J Geophys Res: Atmos 105(D8):10081–10102